INTEGRAL

Science Operations Centre

Announcement of Opportunity for Observing Proposals (AO-4)

SPI Observer's Manual

INT/SDG/05-0244/Dc

Issue 4.0

13th March 2006

Prepared by C. Sánchez-Fernández

Authorised by A. N. Parmar

Based on inputs from:

J.P. Roques, SPI Co-PI, CESR Tolouse

R. Diehl, SPI Co-PI, MPE Garching

Table of Contents

1   Introduction

This document is meant to tell the observers what the SPI (Spectrometer onboard INTEGRAL) instrument is, how it works and how to use it for astronomical observations.

The INTEGRAL payload consists of four instruments, two gamma ray instruments (a spectrometer, SPI, and an imager, IBIS) and two monitoring cameras (an X-ray monitor, JEM-X, and an optical monitor, OMC). Whereas the main scientific goal for the IBIS instrument is high resolution imaging of gamma ray sources with moderate degreee spectroscopic capabilities, the scientific goal for the SPI instrument is high resolution gamma ray spectroscopy with some imaging capabilities in the 20 to 8000 keV range. The SPI instrument is the first high resolution gamma ray spectral imager to operate in this energy range.

The spectrometer SPI has been developed for ESA under the responsibility of CNES Toulouse (France) as prime contractor. Subsystems for SPI have been built by: LDR and MPE (Germany; Anti-coincidence subsystem), the University of Louvain (Belgium; Germanium for detectors), CESR (France; Ge detectors and their electronics), CEA (France; Digital Front End Electronics), CNES (France; cryostat, lower structure, flight software, thermal control), University of Valencia (Spain; coded mask), IFCTR Milano (Italy; Plastic Scintillator) and the University of Berkeley and San Diego (USA; Pulse Shape Discriminator). The instrument has two Co-PIs: J.P. Roques (CESR, Toulouse, France) and R. Diehl (MPE, Garching, Germany).

2   Description of the instrument

2.1   Overall design

The SPI instrument design is based on a hexagonal geometry, which is the most compact one. The instrument is a coded mask spectrometer. The main characteristics of the instrument are given in Figure 1 An overall cut-view of the instrument is shown in Table 1.

Table 1- Main characteristics of the SPI instrument.

Detector dimensions	60 mm wide surface, 70 mm deep
Mask dimensions	665 mm flat to flat 30 mm thick Tungsten
Detector unit	Encapsulated Ge, hexagonal geometry, 19 detectors 70 mm thick
Energy range	18 keV - 8 MeV
Energy resolution (FWHM)	2.2 keV at 1.33 MeV for each detector, 3 keV for the whole spectrometer.
Angular resolution	2.5^o for point sources
Point source positioning	$<1.3^o$ for point sources (depending on point source intensity)
Field-of-View	fully coded: 13.2^o flat to flat, 16° corner to corner zero coding: 30.5^o flat to flat, 35° corner to corner (zero sensitivity)

The detector of the instrument consists of 19 cooled, hexagonally shaped, high purity Ge detectors, providing a total area of about 500 cm^2.

The background on the detectors is limited by use of several methods. An Anti-Coincidence veto System (ACS), consisting of 91 bismuth-germanate (BGO) scintillator blocks, vetos out-of-field photons and particles, and a plastic scintillator underneath the coded mask vetos photons originating in the mask. The veto shield also defines the field-of-view of the instrument, since it vetoes the out-of-field photons. The sensitivity of the instrument is limited by the background due to the primary and secondary cosmic ray particles and the cosmic background radiation. A Pulse Shape Discriminator system (PSD) was aimed at reduction of β-decay background in the Ge detectors; it has been found rather ineffective under real background conditions and is not used.

2.2 The Passive Mask

The passive mask is located at the top of the SPI instrument, above the plastic scintillator. The purpose of the mask is to code the incident gamma rays in the field-of-view, giving the instrument imaging capabilities. The mask also provides stiffness to the primary structure of the SPI instrument.

The mask consists of a sandwich structure made of:
- a nomex honeycomb core covered by two skins,
- a titanium ring that forms the interface to the rest of the instrument
- a coded motif made of hexagonal tungsten blocks that are stuck and screwed onto the sandwich structure.

The tungsten motif provides the specific transparency and geometry for the mask. The mask is made of 127 elements of hexagonal shape and inscribed in a 78 cm diameter circle. Of these elements 63 are opaque and 64 are transparent. Each opaque element is 30 mm thick and 60 mm flat to flat in size. The tungsten elements stop the gamma ray radiation in the range 20 keV to 8 MeV, with an absorption efficiency greater than 95% at 1 MeV. The holes in the mask have a gamma ray transparency of 60% at 20 keV and 80% at 50 keV. The mask is located 171 cm from the detector plane. The distance between the mask and the detector plane is driven by the required field-of-view and angular resolution. The total mass for the mask is 139.4 kg (10 kg titanium, 107 kg tungsten, rest in other materials). A picture of the mask pattern is given in Figure 2.

2.3 The Camera

2.3.1 Cryostat

For an optimum sensitivity and resolution the detectors of the SPI instrument have to be kept at a constant, low temperature of 85 K. The SPI cryostat (which is made of Be) is designed to keep the detectors at this optimum operating temperature. The cryostat is composed of three parts: an active cooling system, a passive cooling system and a cold box. The active cooling system brings the temperature of the cold plate on which the detectors are mounted down to 85 K, using two pairs of cryocoolers. In normal operating mode all coolers work simultaneously. In case of failure of one of the cryocoolers or of the electronics, the instrument will be functional, but in a degraded mode, as the detector temperature can rise to more than 100 K. The detector assembly is placed inside the cold box, which is kept at approximately 210 K by the passive cooling system. All temperatures of the cryostat subsystems are regularly monitored to provide the ground operators with early warnings on failures of coolers, and to provide temperature information that can be used for the data processing.
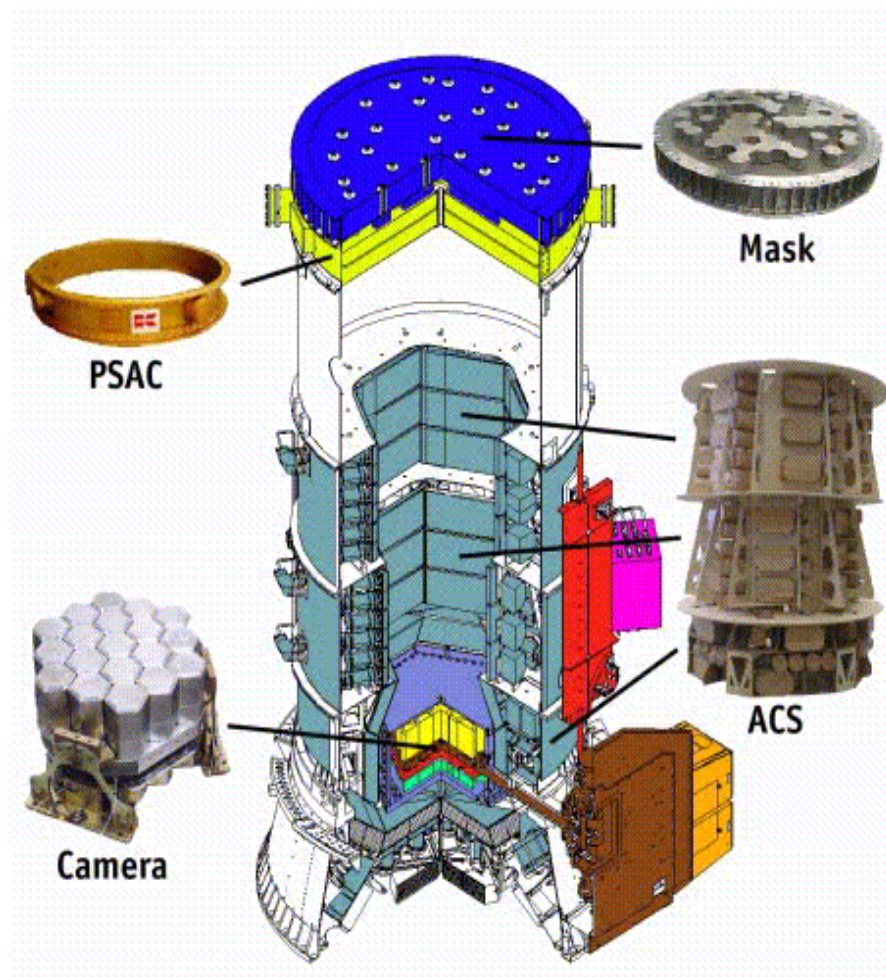
Figure 1- A cut-away view of the SPI instrument. The mask, plastic scintillator, camera and ACS subsystems are highlighted.
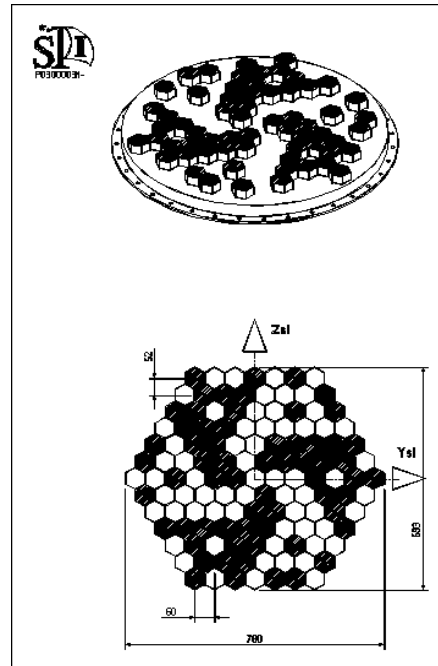
Figure 2 – The passive mask of the SPI instrument. The bottom picture indicates the direction of the spacecraft Y and Z axes with respect to the mask. (See the "INTEGRAL Manual" for the definitions of the axes).

2.3.2 Detectors and pre-amplifiers

The detectors used for SPI are 19 hexagonal-shaped Al encapsulated high purity Germanium detectors, mounted on a cold plate at 85 K, as close as possible together. Currently 17 out of the 19 detectors are operated following failures in December 2003 and July 2004.

The size of the detectors is 5.6 cm, flat to flat, with a height of 7 cm. The hexagonal detectors are mounted with minimum space between them, such that the axes of two adjacent detectors are 6 cm apart.. The cold plate is made of beryllium and it is directly cooled by the SPI cooling system. The bottom of the cold plate is hollowed to mount the printed board pre amplifiers (PA-1) cold electronics. The PA-1 electronics include the high voltage filter and the connection between the detector and the Charge Sensitive Amplifier (CSA). A second set of 19 pre-amplifiers (PA-2) is mounted on a second cold plate (beryllium, at 210 K). The PA-2 is connected to the PA-1 with a cryogenic cable.

The material in front of the detector has good transparency for gamma-rays at 20 keV. To cure the degeneration of the Ge detectors, an annealing operation is performed approximately every 6 months, in which the detectors are heated to 105° C. The instrument will not be available for scientific observations during the time needed for the annealing operation and the cooling phase afterwards (in total 5 revolutions, equivalent to 15 days).

2.3.3 The detector electronics

The signals from the pre-amplifiers are sent to the amplification chain, which is made up of a Pulse Shape Amplifier (PSA) and a Pulse Height Amplifier (PHA). The PSA amplifies the pulses such that the performance of the spectrometer is optimised. This is done by making a compromise between getting the best signal to noise ratio for the pulses, operating in the full 20 keV-8 MeV energy band of the instrument without resolution degradation, and making the output pulses insensitive to the fluctuations in the detector signal rise time. The PHA is used to maintain the energy resolution in the full 20 keV-2 MeV or 2 MeV to 8 MeV range. Finally the detector electronics also comprise a high voltage power supply (0-5000 V) and a low voltage power supply (19 independent chains per amplification chain).

2.3.4 Pulse shape discriminator (PSD)

The PSD subsystem compares the form of the pulses produced by the pre amplifiers with profiles stored in an onboard archive. It was aimed at reduction of β-decay background in the Ge detectors; it has been found rather ineffective under real background conditions and is not used.

2.4 Anti-Coincidence Subassembly (ACS)

The main function of the Anti-Coincidence Subassembly (ACS) is to shield the Ge detectors against background (photons and particles) from sources outside the field-of-view. The ACS system consists of 91 Bismuth Germanate (BGO) scintillator crystals in combination with photo multiplier tubes. The BGO crystal thickness has been optimised with Monte Carlo simulations to minimize the detector background (by minimizing the shield leakage and neutron induced radiation in the BGO). The BGO shield for the side and the rear of the camera is 5 cm thick. The complete shield consists of two collimator rings (that define the SPI field-of-view), located between the mask and the camera unit, a side shield and a rear shield that surround the camera. The BGO scintillator crystals are used to convert all incoming events into photons in the 480 nm region (visible light). Photo-multiplier tubes are used to detect these photons and convert them into electrical pulses which are combined into an overall veto signal. Additionally, the DFEE time-tags these events, and transmits event rates at 50 ms resolution; these can be used, e.g., for gamma-ray burst studies. Photons that occur outside the ACS veto signal are considered, sorted, normalised and summed up by the ACS electronics. Each photon induces a time tagged veto signal. The ACS output data is directed to the Digital Front End Electronics (DFEE) which formats the data and time tags each event. Photons that are not in coincidence with an ACS veto event are considereintegral mand "good". The ACS-off photons (i.e all photons that are detected by the Ge detectors, independent of the veto status) are integrated into background spectra, that are sent to the ground every 30 minutes.

2.5 The Plastic Scintillator Anti Coincidence Subassembly (PSAC)

The purpose of the plastic scintillator subassembly (PSAC) is to reduce the 511 keV background due to particle emission by the passive mask. The detector consists of a plastic scintillator inside a light tight box, located just below the passive mask. It has a good gamma ray transparency, and actively detects particles which deposit energies in excess of 300 keV. The light flashes that are produced by the impacts of these high energy particles are detected with two photo multiplier tubes located around the light-tight box and converted into electrical pulses which are processed by the PSAC electronics assembly. The electronics send a veto signal associated with the detected events and compatible with the Anti-Coincidence Subassembly (ACS) Front End electronics veto signal to the veto control unit of the ACS. Inflight calibrations showed that background reductions through the PSAC are on the order of a few %.

2.6 Electronics

The electronics is divided into the Digital Front End Electronics (DFEE) and the Data Processing Electronics (DPE). The DFEE is in charge of the real time acquisition, assembly, time tagging and synchronizing the various signals from the SPI front end. (detector electronics, PSD, ACS etc.). The DFEE subdivides the events into classes depending on their origin in the instrument (detector electronics, Ge detectors, PSD, veto shield) and handles overall event energies and system monitoring statistics (dead time, signal counts etc.). The detected events are time tagged with a 20 MHz local clock, which provides the timing resolution. The reset (timing reference) is done with the 8 Hz satellite clock. The DFEE uses the 125 ms time frames to analyse and process the input information and pass it on to the DPE. The statistics are passed on to the DPE every second. The DPE is the interface to the instrument. It is part of the On Board Data Handling (OBDH) unit. It provides the telecommand and telemetry interfaces to the instrument and it provides the environment for the instrument dedicated software (Instrument Application Software, IASW).

3 Instrument Operations

3.1 How the instrument works.

The SPI instrument provides a combination of high-resolution spectroscopy with imaging capabilities. The performance characteristics of the instrument each depend on one of the instrumental subsystems:

- Energy resolution: is determined by the cooled Ge detectors
- Angular resolution: is determined by the pixel size of the mask and the detector, and the distance between them. However imaging with SPI requires a special operation (dither) since a single pointing does not unambiguously define a sky image. For this, the 5 by 5 and hexagonal dithers have to be used (see below).
- Field-of-View: determined by the area of the mask and the detector and the distance between them, as well as the ACS shield.
- Sensitivity: achieved by making the detector as large as possible and by minimizing the background (using an ACS that is optimised in material and thickness, by carefully choosing the materials used in the instrument and by adding a plastic scintillator below the mask).

The passive mask provides the shadowgram for image reconstruction. The PSAC detects energetic particles originating in the mask, and provokes a veto pulse from the veto system. The ACS detects gamma rays and charged particles from out of field sources, and also provokes a veto pulse. Each photon that is absorbed in a Ge detector will give a pulse that is sent to the electronics. The electronics analyses the incoming pulses and the veto signals and tags each photon with the energy, the time, and the type of event (i.e. single or multiple detector events). These data are then sent to the ground (see below). The ACS-off photons are summed into background spectra that are sent to the ground every 30-60 minutes.

3.2 Operating modes

The SPI instrument has only one mode for normal observations. All scientific observations with SPI are done in a so called photon by photon mode with a high temporal resolution. In this mode scientific data is collected and transmitted to the ground for each photon. However, due to telemetry limitations, only certain types of detected photons are transmitted directly; the rest is in the detector spectra. For each detected photon, data is sent to the ground from which the type of event, the

energy and the timing can be deduced. Furthermore detector spectra of all events (including vetoed events) can be accumulated and transmitted every 30-60 minutes. In case the SPI telemetry is continuously overflowing due to background radiation that is higher than expected or due to a strong solar flare, the instrument can be operated in a 'degraded' science mode (TM emergency mode). In this case the onboard processing and transmission of data will be restricted to 'good' events (non-vetoed). The maximum data generation rate in this mode will be about half the rate for normal photon by photon mode. The observer cannot select the TM emergency mode, it is commanded by the ground controllers in case of need.

Before any change of mode, the SPI instrument will be put into a special configuration mode. This is the only mode in which changes to the instruments configuration can be made. The instrument will not be taking scientific data when in configuration mode (science telemetry processing is stopped). Several other special modes are available for engineering tasks (e.g. annealing) and for instrument calibrations. They are not of interest to the General Observer.

3.3 Dead time

Due to several causes (e.g. veto signals), the SPI instrument experiences within a normal exposure, a dead time, during which no useful scientific data are collected. However, it depends on several external conditions (e.g. increase of the ACS rate during a solar flare). Experience obtained during AO3 has shown that this dead time is about 15% of the observing time

3.4 Telemetry budget

INTEGRAL uses packet telemetry. Each packet corresponds to 0.44 kbps. Experience obtained during previous A0's revealed that the telemetry needed for the operation of the SPI instrument was higher than expected on the basis of model calculations (mainly due to a higher background than expected). Since July 2004 the telemetry allocation for SPI is 103 packets per cycle.

3.5 Spectroscopy and timing

In the standard observing mode the instrument can be used for spectroscopy and timing observations. Since every photon is tagged with an accurate time (see section "Timing capabilities" on page 21 for the timing accuracy). These data can also be used for timing analysis.

It is expected that the background in each of the 19 (17 currently operational) independent detectors will vary in time in a different way. This variation can limit the sensitivity that is obtainable. Several types of background variations can be anticipated:
   • short-term variations due to solar activity and solar system "weather".
   • variations over the orbital period (related to the position of INTEGRAL in the orbit).
   • long-term variations over the mission duration (e.g. solar cycle).

In order to reconstruct the image on the detectors for all pixels in the field-of-view for a single pointing, a set of 19 (currently 17) equations with 156 unknowns would need to be solved. This is impossible, and the only way to increase the number of equations and make the system solvable is to observe more pointings. Thus, in order to solve this problem of background determination an appropriate dithering strategy has to be adopted for every observation (see also the *"INTEGRAL Mission Overview"* Manual). Dithering is also important to improve the image quality of reconstructed sky images. The dithering strategy that has to be adopted depends on the circumstances:
   • observations of a region of multiple or complex sources or of sources with poorly known position. In this case the 5 by 5 rectangular dithering pattern should be used, where 25 points on a rectangular grid with 2° spacing around the source position are observed.

- observation of a single point source of known location, where there are no known other objects of significant intensity in the field-of-view (fully and partially coded, for all dithering points, i.e. within a radius of about 20°). In this case the hexagonal dithering pattern can be used, where a hexagonal scan is performed with one pointing centred on the source, surrounded by six pointings with distances of 2°. Note that the number of sources for which this dithering pattern can be used is very limited, and a justification in the proposal for this mode is required. Ususally only when observing a single strong emission line an hexagonal pattern can be justified.

Both dithering patterns use a dwell time of ~30 minutes per point. This range is optimised for the instrument performance and expected background variations, while the exact duration is calculated to sample the dither pattern an integral number of times.

All SPI observations should use dithering, since reconstruction for pointed observations is very difficult, if not impossible, due to background inhomogeneities over the detector plane (see above). The observer should be aware that polarimetry is not supported.

3.6 Imaging

The imaging performance of SPI depends also on the dithering pattern that is used. In general the greater the number of pointings, the better the imaging. Calculations were done to estimate the imaging performance of the instrument using simple correlation mapping. More sophisticated techniques may be used to improve on removal of artifacts and/or on source sensitivity by better modelling of background and simultaneous analysis for a number of point sources plus diffuse emission; these are beyond the scope of this manual. However, when using the hexagonal dither pattern, the reconstructed point source response function shows very strong side lobes at distances of 10° to 20° from the centre. Therefore this mode should only be used for isolated point sources and is not really suitable for imaging. Experience obtained during previous AO's has revealed that there are not many isolated point sources (sometimes due to e.g. transients) and observers are in general discouraged to use this mode.The side lobes are still present, but significantly less with the 5 by 5 dither pattern (about 50% of the hexagonal case). To remove these side lobes, which will cause artifacts in reconstructed images, the only possibility is to enlarge the imaged area by observing multiple pointings (i.e. multiple dither patterns). In AO3 a slight modification to the standard 5 by 5 dither pattern was used to improve the image reconstruction: the centre of the dither pattern moved between repetitions of the dither pattern by at most +/- 1.27 degree. Additionally a rotation of the instrument FOV by +/- 3 degree was applied in a random way.

3.7 Gamma-ray burst detection

The ACS system of SPI detects gamma ray photons from a large part of the sky during all observations. It can thus work as a gamma ray burst monitor. Because of the size of the ACS BGO shield it has a high sensitivity for gamma ray bursts. Experience obtained during the mission shows that the ACS detects about 2.5 gamma ray bursts per day (minimal detectable energy flux between $4 \cdot 10^{-7}$ erg cm^{-2}s^{-1} and $7 \cdot 10^{-7}$ erg cm^{-2}s^{-1}).

Unfortunately the ACS data cannot be directionally sensitive, therefore accurate positions of gamma ray bursts that are detected with the ACS have to be determined through triangulation methods, with other (distant) spacecraft (e.g. Ulysses). About 400 ACS bursts have been investigated, more than 50% of them being confirmed through triangulations with other spacecraft detectors (Rau et al. 2005).

The INTEGRAL Science Data Centre (ISDC) checks the stream of veto count rates automatically. If a gamma ray burst is detected (sudden increase in the count rate over a short period of

time), an alert is issued to the institutes that are doing the triangulation observations (4th Interplanetary Network). From the accurate timings of the SPI detection and detections by other spacecraft a position is constructed and communicated to the world. The accuracy that can be achieved with this method is much better than an arcminute (due to the long baseline, and the accurate timing of the SPI ACS events). Note that the ACS events are written to the instrument Housekeeping and are therefore made public immediately.

Observers can be notified of these gamma ray burst events by subscribing to the gamma ray burst alert system of the INTEGRAL Science Data Centre (see also the INTEGRAL manual).

GRBs can of course also be detected in the SPI field-of-view using the normal photon-by-photon mode. In this case the data belong to the observer who has an accepted proposal for GRBs in the FOV (see also the document *"INTEGRAL Science Data Rights"*). A gamma ray burst in the field-of-view occurs about once per month.

4   Performance of the instrument

4.1   Components and sources of instrumental background

The SPI instrument is background limited. The sensitivity of the instrument is therefore largely dependent on the background and on the correct identification of background photons. The background can be divided into the following main components:
- continuum radiation
- 511 keV line radiation
- gamma ray lines

In the following subsections we will describe each of these components separately.

4.1.1   Continuum background

The continuum background can be split into several components, depending on their origin. First the radiation coming from outside the instrument. This can be the cosmic diffuse gamma ray flux that comes in through the instrument aperture, or leakage through the BGO shield of cosmic diffuse gamma ray radiation and gamma continuum radiation from the spacecraft (induced by energetic cosmic ray particles). Secondly, scattering in the Ge detectors of neutrons that were produced in the spacecraft or other parts of the instrument. Thirdly background components produced inside the spectrometer detectors. These consist of localised β^- decays, non localised β^- decays and β^+ decays. About 90% of localised β^- decays (single events) are identified by the pulse shape discriminator system. The non-localised β^- decays (multiple interactions in the detector, e.g. Compton scattering and photoelectric interaction) are more difficult to identify, since in this case the electron and the gamma photon are emitted simultaneously, therefore the resulting pulse looks like a normal 'source' event for the PSD. The continuum emission from the mask and the BGO emission when the veto electronics are blacked out (veto "dead time") are negligible. The individual components and the total continuum background emission are illustrated in Figure 3.

4.1.2   511 keV background

The 511 keV background can be split into five components:
- the continuum background 'under' the 511 keV line. This component is estimated from the continuum background spectrum as explained above.
- passive material: 511 keV photons are emitted from passive material, due to β^+ decays of unstable nuclei in these materials. These unstable nuclei are formed due to interactions of protons and neutrons that are produced in interactions of cosmic ray particles with the detectors,
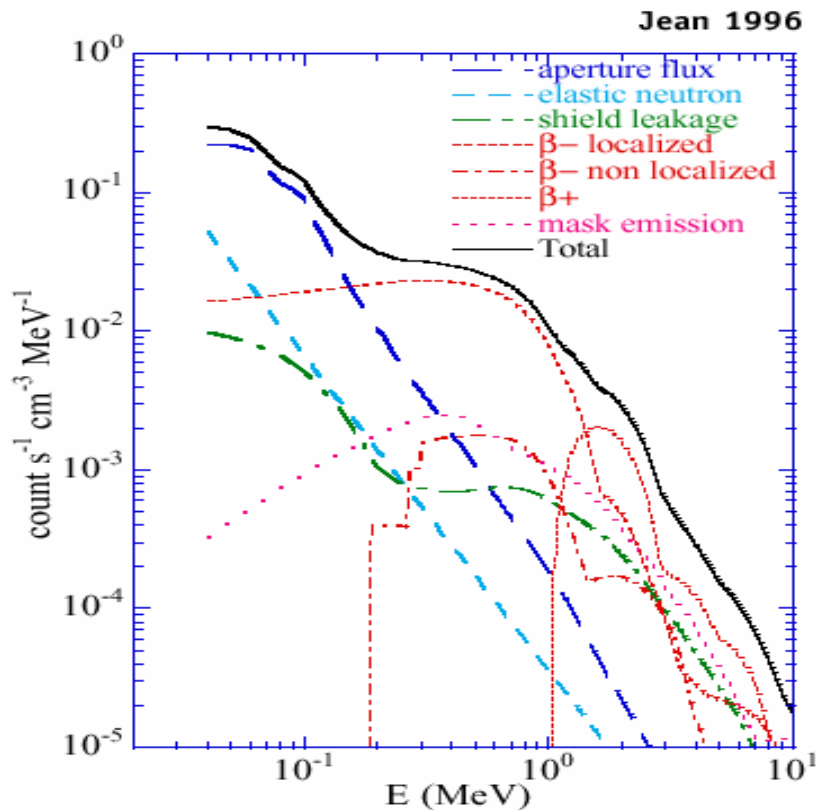
Figure 3 – The continuum background components for SPI. The individual components are identified. The total background spectrum is indicated with the black line. The figure is only indicative: later calculations show a higher total flux above 700 keV.

shield or cryostat. The unstable nuclei decay through β^+ decay. The annihilation of the positron leads to the emission of two 511 keV photons in opposite directions. If one is absorbed by the detector and the other escapes, a 511 keV background event is produced.

• shield leakage: 511 keV photons, originating from interactions of cosmic rays with passive spacecraft materials, that are not rejected by the BGO shield.

• mask component: 511 keV photons originating from cosmic ray interactions with the mask material. The main source is pair creation by cosmic ray proton interactions with W nuclei. This component is reduced by about 8% with the Plastic Scintillator.

• BGO shield blocking time component: 511 keV photons produced by β^+-decays in the BGO shield when the ACS electronics is blocked by a large energy deposit and the veto is on.

All these components were calculated with a Monte Carlo method.

4.1.3 Background gamma-ray lines

Background gamma-ray lines are emitted in passive materials close to the detectors and in the detector material itself. Primary and secondary cosmic ray particles (protons and neutrons) induce excited nuclei in nuclear reactions with nuclei of the passive material. The prompt or delayed (radioactive) de-excitation of these nuclei leads to gamma-ray lines which can be detected by the germanium detectors. Experience shows that lines originating in the mask do not pose a problem for SPI. In Figure 7 (the narrow-line sensitivity) the background lines can be clearly seen, since they affect the sensitivity.
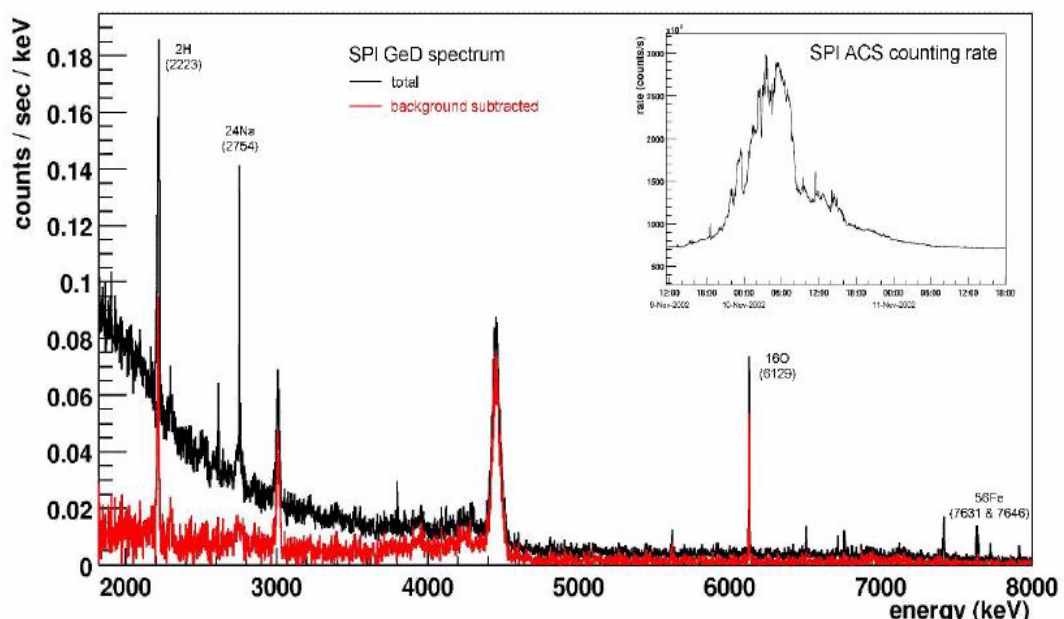

Figure 4 – Example spectrum taken during a solar flare (see inset in top-right), indicating the ability to resolve lines

4.2 Instrumental characterisation and calibration

The SPI instrument has been fully tested and calibrated on ground before the launch. Some tests and calibrations with radioactive sources have been performed on ground with the full satellite. Further testing has been performed during the PV-phase of the mission.The sensitivities, resolution, and other characteristics given in this document are the result of the analysis of the PV- phase observation and other calibration observations. They represent the current best knowledge of the SPI instrumental characterisation.

After launch the SPI team has verfied that the pre-launch calibration, as established on ground, has been maintained. This has been done during the initial in orbit phase (Commissioning Phase) and during subsequent regular observations of the Crab which are used to monitor the status of the calibration. They are carried out during each visibility period of the source, i.e. twice per year. These allow measuring the imaging performance, spectroscopic performance, background characteristics, flux calibration (sensitivity) and the off-axis response. Currently calibration observations of the Crab nebula and Cygnus X-1 have been used to provide the calibration that will
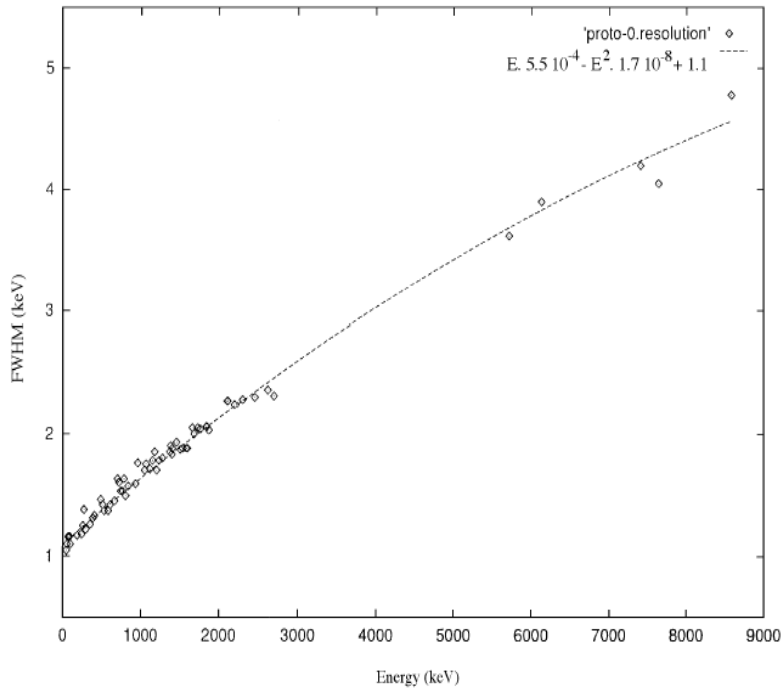
Figure 5 - The measured energy resolution of an individual SPI detector. This was measured using laboratory detectors. The resolution of the full instrument with all 19 detectors is slightly lower than this.

be used for the data processing. The observations of Cygnus X-1 have provided an accurate calibration up to ~ 2MeV, confirmed by the Crab observations. Regular observations of the Crab are used to monitor the status of the calibration.

Also lines originating in the BGO shield (511 keV, 6.1 MeV O line) can be used for calibration purposes (e.g. energy calibration), and lines that originate from materials inside the cryostat that have known intensities can be used to measure the Ge detector efficiency. The detector gains, thresholds and resolution versus energy are determined from normal event data and ACS off spectra (for consistency checks) in the routine monitoring task of ISDC. Finally, after every detector annealing (the first one was performed in February 2003) a thorough check has been done of the instrument imaging and spectroscopic response, since these may change as a result of the annealing process. Up to date seven annealings have been performed which all increased the resolution as expected. The succes of the annealing depended on the length of the annealing cycle: it was found that about 100 hours of annealing were necessary to restore the full resolution to close to pre-launch values. Experience obtained during the early mission has also revealed that using the information from the PSD does not significantly increase the signal to noise ratio and is therefore currently not used in the analysis.

4.3 Measured performance

4.3.1 Imaging resolution

The measured angular resolution for (isolated) point sources is about 2.5^o (FWHM).This is the measured width of the instrument response correlation for a point source. The location of point sources can be done with an accuracy better than this, but this depends on the strength of the source.
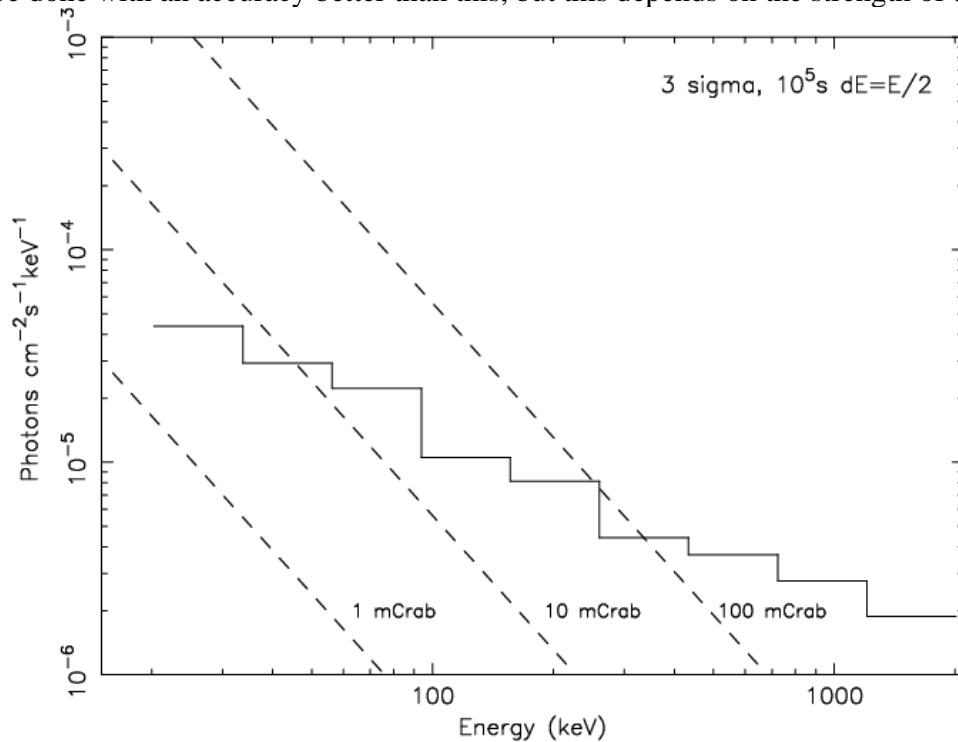

Figure 6 - The continuum sensitivity of the SPI instrument for a 3 sigma detection in 10^5 seconds on-axis. Fluxes are for E=E/2. The dashed lines indicate extrapolation from X-rays using a power law with photon index -2.1 for 1, 10 and 100 mCrab. Corrections for failures of detector elements and source aspect angle and dithering must be applied (see Sect. 5.3.2 and 5.3.3).

As explained above, dithering is required for SPI, especially for regions with more than one source or diffuse emission. Positions obtained from SPI have an uncertainty, which is mainly statistical and therefore countrate dependent. The uncertainties decrease as the inverse of the detection significance, and range from ~10 to ~1 arc minute for detection significances of ~10 to ~100. For higher detection significances (e.g. the Crab) the detection is ultimately limited to ~0.5 arcmin in position.

4.3.2 Spectral resolution

The spectral resolution has been measured in the laboratory with detectors that are representative of the flight units, and afterwards with flight model detectors and pre- amplifiers. An example spectrum measured inflight is shown in Figure 4. The measured energy resolution as a function of energy for an individual detector is given in Figure 5. The energy resolution for the full instrument is given in Table 2.

The energy resolution slowly degrades as a function of time by about 20% in 6 months as a

result of radiation damage in the Ge crystals induced by cosmic particles. The damage is not permanent and can be corrected by the annealing procedure, which is foreseen to take place about every 6 months. Annealings have been performed in February 2003, July 2003, November 2003, June 2004, January 2005, June 2005 and January 2006. The evolution of the resolution can be seen in Figure 9. Calibrations are routinely performed on a per-orbit time scale. This is adequate for most purposes (better than 1 keV), but for fine spectroscopy, additional calibrations accounting for degradation and temperature changes may be required. The obtained absolute precision of the energy calibration is about 0.1 keV in the 500 keV to MeV range, while a relative accuracy of 0.01-0.02 keV can be reached. The continuum and line sensitivities of the SPI instrument are given in Figure 6 and Figure 7.

Sensitivities for continuum and narrow lines are shown in Figure 6 and 7, respectively; values are at 3 sigma significance, for 10^6 sec integration time, using the normal operating mode and all event types (SE+ME) combined. Note that in regimes of strong instrumental lines (such as the 511 keV line), sensitivities can be significantly worse than between such lines. For broad lines, sensitivity degrades due to more background being included, as shown in Figure 8

Two of the 19 detector units have been lost: Detector #2 in Dec 2003, and #17 in Jul 2004. This implies loss of single events from these detector units, and increased single-event rates in neighboring detectors from the former multiple-events of #2 and #17 (scattering into neighboring detectors). The sensitivity loss thus depends on event type selection, and amounts to between 5% for continuum and 20% for low-energy lines. The sensitivity figures (Fig. 6,7) are for the 19-element Ge camera, hence do not include these effects.

Table 2 – The energy resolution (FWHM), continuum and narrow line sensitivities of the SPI instrument (3-σ detection in 10^6 seconds). Note that the line sensitivities can be a very strong function of energy close to the lines (See Figure 7). The continuum sensitivities are for $\Delta E = E/2$. Corrections for failures of detector elements and source aspect angle and dithering must be applied (see Sect. 4.3.2 4.3.3).

Energy (keV)	Resolution (keV)	Continuum sensitivity (ph cm-2s-1keV-1)	Line sensitivity (ph cm-2s-1)
50	1.53	9.2 10-6	5.6 10-5
100	1.56	3.3 10-6	3.3 10-5
500	1.93	1.2 10-6	2.3 10-5
1000	2.21	8.8 10-7	2.4 10-5
5000	3.62	1.4 10-7	1.1 10-5

4.3.3 Off-axis sources and dithering

Above sensitivities are derived for a source on axis. The SPI sensitivity varies with incidence angle as shown in Tab. 4; corrections should be applied accordingly. SPI observations are normally taken by systematically varying the pointing axis around the target of interest. This allows for a determination of the instrumental and diffuse background, as the source shadowgram is displaced in a systematic way. For isolated point sources, a "hexagonal dither pattern" is suitable to always align the source shadowgram with detector elements. A normal 5 by 5 grid pattern is used for observations where more sources are in the (large) field of view. When using a HEX dither pattern, users should assume a 20% reduction in sensitivity compared to Figures 6 and 7.
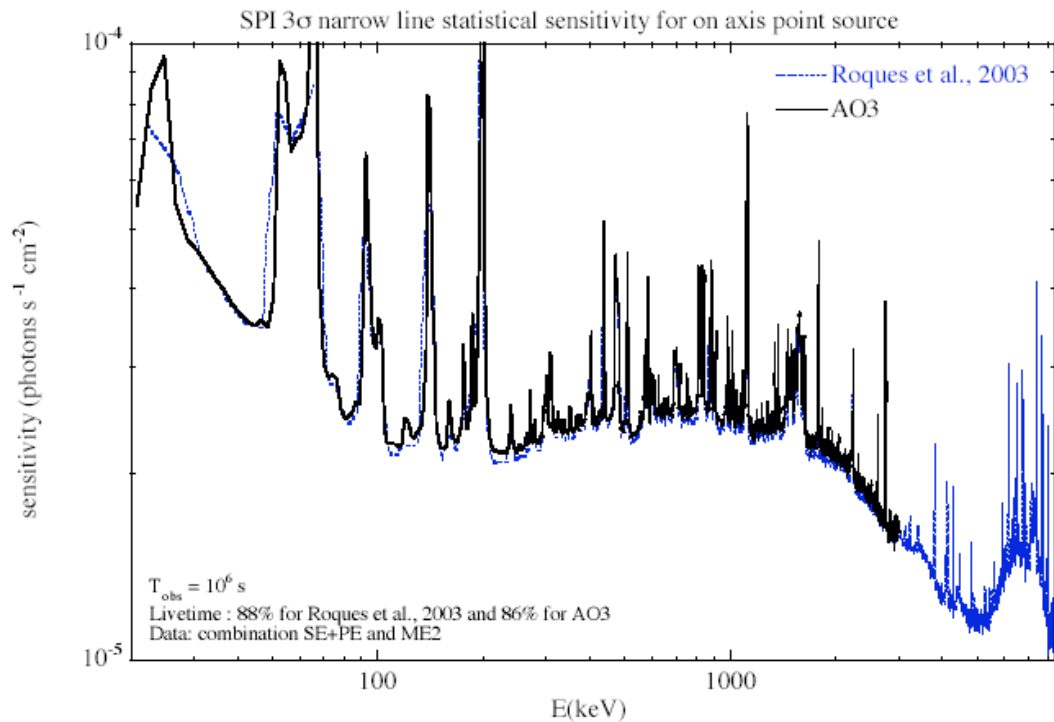
Figure 7 - The narrow line (w.r.t. the instrument resolution) sensitivity of the SPI instrument for a 3-σ detection in 10^6 seconds. Corrections for failures of detector elements and source aspect angle and dithering must be applied (see Sect. 5.3.2 and 5.3.3).

4.3.4 Imaging capabilities

Above sensitivities are valid for sources with known position. For source searches, the number of independent trials in a mapping analysis must be accounted for. At an effective point spread function width of 2.5 degrees, this corresponds to about 60 independent trials for a 25 x 25 degree map.

With this effective PSF extent of 2.5 degrees, imaging location of sources depends on source significance above background and locations of nearby sources: Strong sources can be located to an accuracy of 0.5 arcmin, while sources closer than 2 degrees will not be discriminated though imaging (see Dubath et al. 2005; MNRAS, 357, 420). Combination of observations allows for imaging of large sky areas, as has been shown for continuum and 511 keV line emission (Strong et al. 2005; A&A. 444, 495 ; Knoedlseder et al. 2005; A&A, 441, 513).
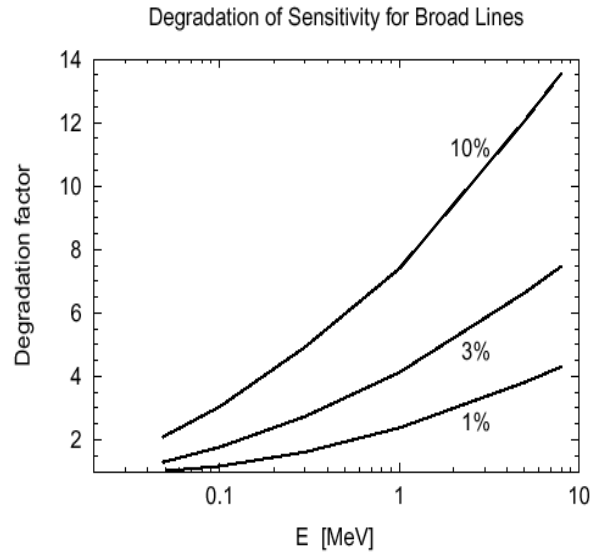
Figure 8- The degradation factor or the line sensitivity for broad lines (with a width of 1, 3 and 10 % of the line energy) as a function of energy.

Table 3 - Sensitivity degradation factor as function of the distance off-axis for a hexagonal and a 5 by 5 dither pattern.

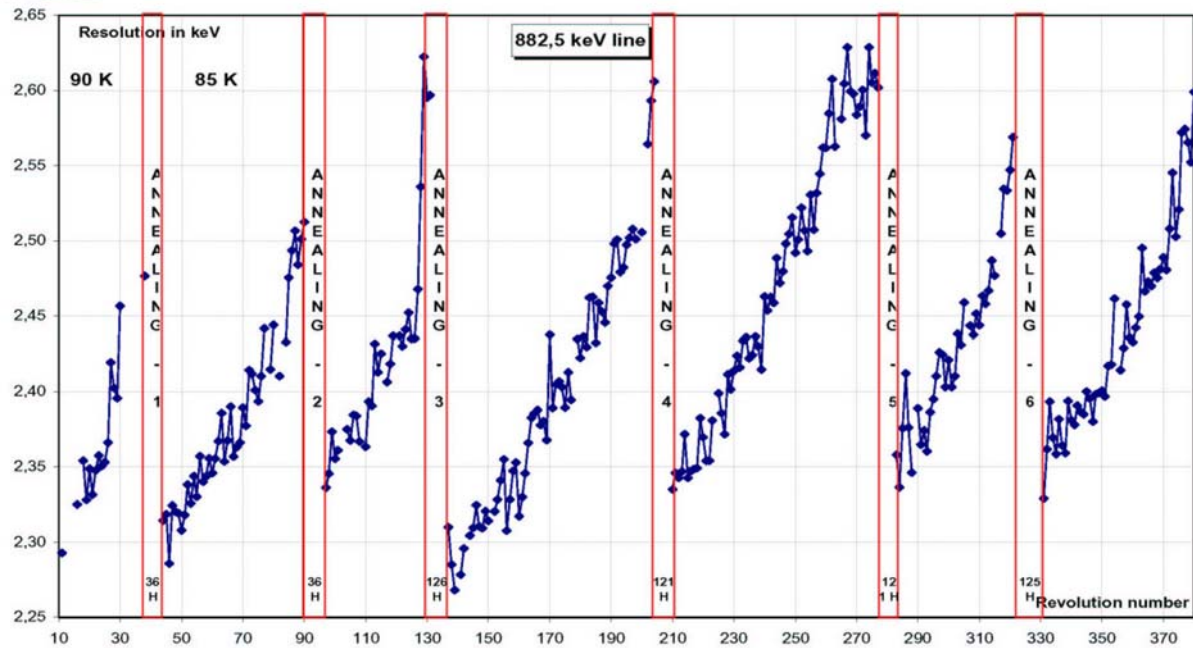| Off axis distance (degrees)	Sensitivity degradation	
	hexagonal	5 by 5
0	1.0	0.8374
1	0.6655	0.7925
2	0.7638	0.8004
3	0.6838	0.7879
4	0.7147	0.7874
5	0.7056	0.7746
7.5	0.6309	0.7357
10	0.5505	0.6718
12.5	0.4938	0.5918
15	0.3749	0.5002
17.5	0.1888	0.3774
20	0.0886	0.2047
25	0.0	0.0148
30	0.0	0.0

Figure 9 - The evolution of energy resolution at 882.5 keV as a function of time in-between the annealing periods.

4.3.5 Timing capabilities

The instrument works in photon by photon mode. Each photon data set includes timing infor-mation given by a 100 μs clock signal. This clock is synchronised to the on board clock, and thus to the UTC. The timing error budget for SPI is derived from:

- the accuracy of the onboard clock and the synchronisation,
- the conversion between onboard time and UTC,
- the conversion between UTC arrival time at the spacecraft and the arrival time at the solar system barycentre.

The resulting SPI timing accuracy calculated in this way is 129 μs, 3σ accuracy, and a 90% confi-dence accuracy of 94 μs. A timing analysis of the Crab data has revealed that the absolute timing accuracy is about 40 μs (1σ uncertainty). Note that during AO-1, a part of observations were taken in a 'histogramming' mode, reducing timing accuracy to ~30 min; therefore, in combining new observations with data from the 2002/early 2003 period, proper operation mode data must be selected.

5 Observation "Cook book"

5.1 Astronomical considerations on the use of the instrument

The SPI instrument is designed as a spectrometer, therefore it should primarily be used for high resolution spectroscopy on sources with (narrow) lines, possibly on top of a continuum. Given the imaging qualities of the instrument it can also be used for wide field imaging of diffuse emission, especially in (narrow) emission lines. However if high resolution imaging, or observations of sources with only continuum emission or very broad lines are needed, the IBIS instrument might be better suited as prime instrument, at least below a few hundred keV.

The prime astrophysical topics to be addressed with SPI are nucleosynthesis processes, super-nova theories, nova theories, interstellar physics and pair plasma physics in compact objects (neutron stars, black holes). A number of interesting lines fall in the SPI energy range. Table 4 gives a list of some lines and energies.

Table 4 - Some gamma ray lines from cosmic radioactivity in the SPI energy range.

isotope	decay chain	line energies (MeV)	Mean life (year)
e^+	$e^+ + e^-$ photon	0.511	~1 10^5
^{56}Co	$(^{56}$Ni$)$ ^{56}Co ^{56}Fe	0.847 1.238	0.31
^{22}Na	^{22}Na ^{22}Ne	1.275	3.8
^{44}Ti	^{44}Ti ^{44}Sc ^{44}Ca	1.156	89
^{26}Al	^{26}Al ^{26}Mg	1.809	1.0 10^6
^{60}Fe	^{60}Fe ^{60}Co ^{60}Ni	1.173 1.322	2.2 10^6

5.2 How to estimate observing times

The formal way to calculate accurate observing times is via the Observing Time Estimator(OTE).

OTE can be found on

http://integral.esac.esa.int/isoc/operations/html/OTE.html

In this section however we give an easy way for observers to estimate the observing times using simple formulae. The times that are calculated in this way are reasonably accurate, and are for most cases within a few percent from the OTE calculated times. In the worked examples we give both times for comparison. Note that the ISOC will only use the OTE to assess the technical feasibility of proposals.

General observers can request to observe a gamma-ray line flux (in photons $cm^{-2}s^{-1}$) or an integrated continuum flux over an energy band (also in photons $cm^{-2}s^{-1}$) at a given energy from a point source.Therefore, two types of observation time calculation will be presented in the following sections. The continuum sensitivity can be estimated using the narrow line sensitivity, the energy resolution and the energy-band required. In the Proposal Generation Tools, PGT, a line has to be given in as a narrow energy range with the width of the line. The inputs to both OTE and PGT for continuum are for an in-band flux, and since the sensitivities are for $\Delta E = E/2$, the band over which

the flux is specified should not be too broad (maximum $\Delta E = E/2$) to perform calculations. However, with the latest version of OTE one can specify a power-law slope and OTE will split the total energy band up into many small bands and combine the results. The observers should make sure that observing times entered into PGT allow the completion of at least one full dither pattern (i.e. minimum of 12600 seconds for hexagonal dithers and 45000 seconds for 5 by 5 dithers).

5.2.1 Gamma-ray line

The observation time, T_{obs} (in kilo seconds), is estimated using the relation

$$T_{obs} = 1 \cdot 10^3 \left(\frac{N_\sigma}{3} \cdot \frac{S_{line}}{F_{line} \cdot Frac} \right)^2 \cdot \frac{\Delta E}{R} \cdot \frac{1}{1 - f_{dead}}$$

where:

- N_σ is the number of sigma required.
- S_{line} is the 3σ, point source on-axis, narrow line sensitivity for SPI at the considered energy and for 10^6 s and a lifetime of 100%. The values of this parameter are in Table 2.
- F_{line} is the source line flux in ph/s cm^2.

Frac is the sensitivity degradation factor due to the dithering or the source being off-axis. See Table 3 and section " Off-axis sources and dithering" on page for details.

- ΔE is the width of the expected gamma-ray line (FWHM in keV).
- R is the energy resolution of the spectrometer (in keV). It depends on the energy, the values of this parameter are in Table 2.
- f_{dead} is the fraction of dead-time (12%). This parameter is described in section "Dead time" on page 11 .

5.2.2 Gamma-ray continuum

The observation time, T_{obs} (in kilo seconds), is estimated using the relation:

$$T_{obs} = 1 \cdot 10^3 \left(\frac{N_\sigma}{3} \cdot \frac{S_{line}}{F_{int} \cdot Frac} \right)^2 \cdot \frac{\Delta E}{1.5R} \cdot \frac{1}{1 - f_{dead}}$$
$$= 1 \cdot 10^3 \left(\frac{N_\sigma}{3} \cdot \frac{S_{cont}}{F_{cont} \cdot Frac} \right)^2 \cdot \frac{E}{2\Delta E} \cdot \frac{1}{1 - f_{dead}}$$

Where:

- F_{int} is the flux integrated over the specified band (in ph/cm^2s)
- F_{cont} is the continuum flux in the specified band (in ph/cm^2s keV)
- ΔE is the width of the energy band corresponding to the specified flux (in keV)
- S_{cont} is the continuum sensitivity as given in . The continuum sensitivity can be calculated from the line sensitivity using:

$$S_{cont} = S_{line} / (\sqrt{1.5R \cdot \Delta E})$$

All other parameters are as described above. The factor 1.5 is used to correct the gamma-ray line sensitivity that is calculated assuming that the total counts in a line are contained in an energy band of 1.5 times the spectral resolution (FWHM). Actually, 1.5 times the resolution contains ~95%

of the line counts..

5.3 Worked examples

In this section we present some examples of observations with SPI for which we calculated the observing times with the formulae given above and the Observing Time Estimator. Note that for lines, the exposure time derived from OTE differs from the one calculated from the formula. This is because OTE uses sensitivities at a much higher energy resolution than tabulated in Table 2 (see Figure 7). The examples below (for lines) are therefore only intended as an order of magnitude estimate; one should use the exposure times obtained with OTE.

Example 1: a line at 1809 keV (^{26}Al), with a 3 keV width, and a integrated line flux of 5×10^{-5} ph cm^{-2}s^{-1}, observed with a 5 by 5 dither pattern. The requested significance is 3 sigma. The sensitivity at this energy is 2.1 10^{-5} ph cm^{-2}s^{-1}, the resolution is 2.553 keV, and the sensitivity degradation factor for a 5 by 5 dither is 0.8374. Using these numbers the required observing time would be 224 ksec or 2.59 days (OTE gives 493 ksec).

Example 1a: (to show the correspondence between manual and OTE results at an energy where the line sensitivity is fairly constant) a line at 2000 keV, with a 3 keV width, and a integrated line flux of 5×10^{-5} ph cm^{-2}s^{-1}, observed with a 5 by 5 dither pattern. The requested significance is 3 sigma. The sensitivity at this energy is 2.0 10^{-5} ph cm^{-2}s^{-1}, the resolution is 2.634 keV, and the sensitivity degradation factor for a 5 by 5 dither is 0.8374. Using these numbers the required observing time would be 295 ksec of 3.41 days (OTE gives 337 ksec).

Example 2: the same 1809 keV line, but now observed with a hexagonal dither (sensitivity degradation factor 1.0) would for a significance of 3 sigma require 157 ksec, or 1.82 days (however, this mode is only applicable for isolated point sources) (OTE gives 346 ksec).

Example 3: a continuum band of 150 keV width, centred at 350 keV, with a continuum flux of $2 \ 10^{-5}$ ph cm^{-2}s^{-1}keV^{-1}, observed with a 5 by 5 dither for a significance of 10 sigma. The continuum sensitivity for this energy is 1.4 10^{-6} ph cm^{-2}s^{-1}keV^{-1}, the resolution is 1.80 keV and the sensitivity degradation factor is again 0.8374. This observation would then require 103 ksec, or 1.19 days (OTE gives 102 ksec with an in-band flux of 3.0 10^{-3} ph cm^{-2}s^{-1}).

Example 4: the ^{44}Ti line (at 1.160 MeV) in a supernova remnant (e.g. Cas A). The line width is 2000 km/sec (or 7.73 keV), the integrated line flux $1 \ 10^{-4}$ ph cm^{-2}s^{-1}. The source should be observed with a 5 by 5 dither, for a significance of 5 sigma. The sensitivity of the instrument at this energy is 2.4 10^{-5} ph cm^{-2}s^{-1}, the resolution is 2.28 keV, and the sensitivity degradation factor is again 0.8374. The required observing time for a significance of 5 sigma would then be 586 ksec or 6.78 days (OTE gives 861 ksec).

Example 5: a broad, red shifted 511 keV line. The energy of the line is 470 keV, with a width of 5000 km/sec (or 16 keV), and a integrated line flux of $3.3 \ 10^{-4}$ ph cm^{-2}s^{-1}. The observation should be in hexagonal dithering mode (isolated source), for a significance of 5 sigma. The sensitivity of the instrument at this energy is $4.6 \ 10^{-5}$ ph cm^{-2}s^{-1}, the energy resolution is 1.93 keV and the sensitivity degradation factor is 1.0. This observation would then take 347 ksec, or 4.02 days (OTE gives 274 ksec).

Example 6: a continuum band of 500 keV width, centred at 4 MeV, with a continuum flux of $1 \ 10^{-6}$ ph cm^{-2}s^{-1}keV^{-1}. The observation should use a 5 by 5 dither pattern, and achieve 3 sigma on source. The sensitivity of the instrument is $1.4 \ 10^{-7}$ ph cm^{-2}s^{-1}keV^{-1}, the resolution is 3.32 keV and the sensitivity degradation factor is 0.8374. This observation would require 172 ksec, or 2.0 days (OTE gives 698 ksec, assuming a constant photonflux over the energy band, giving an in-band flux of $5 \ 10^{-4}$ ph cm^{-2}s^{-1}).

Example 7: an extended source with a size of 4.8 arc minutes and a continuum flux in a band of 150 keV centered at 350 keV of $2 \ 10^{-5}$ ph cm^{-2}s^{-1} keV^{-1}. With an angular resolution of 2.5 degrees, the source can be resolved in $(4.8/2.5)^2$ pixels. In 102 ks a sensitivity of $10/(4.8/2.5)$ (see example 3) or 5.2 sigma can be reached.